ACS APPLIED NANO MATERIALS

Open Access

www.acsanm.org

Article

Sulfur-Enriched Nanoporous Carbon: A Novel Approach to CO_2 Adsorption

Chen Liu, Yue Zhi, Qiyun Yu, Lifeng Tian, Muslum Demir,* Suleyman Gokhan Colak, Ahmed A. Farghaly, Linlin Wang, and Xin Hu*

Cite This: *ACS Appl. Nano Mater.* 2024, 7, 5434−5441

Read Online

ACCESS | Metrics & More | Article Recommendations | Supporting Information

ABSTRACT: Carbon dioxide (CO_2) intake plays a vital role in sustaining the environmental balance by influencing global carbon dynamics and climatic stability. This work addresses the production of sulfur-doped porous nanocarbons (SDCs) as prospective sorbents for CO_2 capture. SDCs were fabricated by utilizing coconut shell as a carbon precursor and potassium persulfate as both a chemical activating agent and a sulfur dopant. The incorporation of sulfur functionalities into carbon matrices creates structural variability and active sites, boosting CO_2 absorption capabilities. Sulfur's peculiar electrical structure allows greater intermolecular interactions with CO_2, enhancing adsorption affinities. According to the experimental data, the CO_2 uptake was best measured as 3.37 mmol/g at 0 °C and 1 bar and 2.56 mmol/g at 25 °C and 1 bar. The results show that the higher porosity of SDC materials adds to a large amplification in the CO_2 uptake capability. The work underlines the delicate interaction between sulfur doping, morphological porosity, and surface reactivity in enhancing the effectiveness of CO_2 sequestration. SDC materials hold considerable promise in tackling the present ecological concerns and developing CO_2 collection techniques. The suggested single-step synthesis technique described here provides a sustainable and environmentally friendly method for synthesizing SDCs for carbon capture applications.

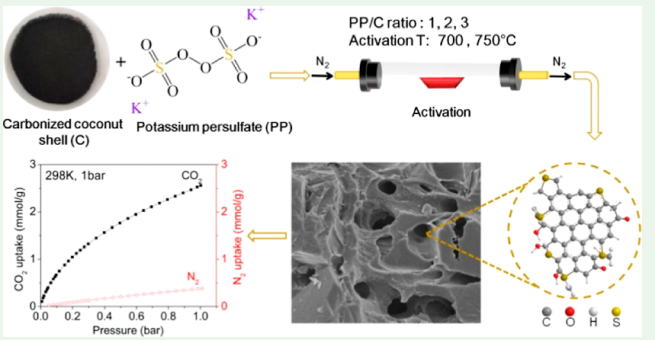

KEYWORDS: *porous nanocarbons, S-doping, CO_2 adsorption, biomass, potassium persulfate*

1. INTRODUCTION

CO_2 uptake is pivotal for the maintenance of environmental equilibrium, encompassing diverse mechanisms through which CO_2 is absorbed from the atmosphere and integrated into various reservoirs, ultimately influencing global carbon dynamics and climate stability.[1] The principal biological mechanism driving CO_2 sequestration is photosynthesis, whereby autotrophic organisms, predominantly plants, assimilate CO_2 as a substrate for the synthesis of organic compounds, thus facilitating plant growth and development. This process not only underpins terrestrial ecosystems but also contributes to carbon sequestration as organic matter accumulates within vegetation and soils. Furthermore, oceanic CO_2 dissolution engenders chemical reactions leading to the formation of bicarbonate ions, with cascading effects on marine ecosystems and oceanic carbon cycling. These complex biological and chemical processes synergistically regulate atmospheric CO_2 concentrations.[2,3]

In the past decade, substantial research efforts have been directed at exploring solid adsorbents, such as carbons,[4−15] metal−organic frameworks (MOFs),[16,17] zeolites,[18] covalent-organic frameworks (COFs),[19,20] and porous polymers,[20−23] for the objective of CO_2 removal. Within this broad spectrum of adsorbents, porous carbons have received great attention due to their potential as very promising sorbents for the extraction of CO_2. This heightened attention is a result of their advantageous characteristics, which encompass a remarkable specific surface area, robust thermal and chemical stability, mild adsorption conditions, cost-effective production methods, facile regeneration processes, minimal energy consumption, and environmentally friendly attributes. These combined qualities underline the potential usefulness of porous carbons in tackling CO_2 collection difficulties, putting them as a focus point in continuing research initiatives.[24−28] Recent investigations have indicated that the insertion of nitrogen (N), sulfur (S), or oxygen (O) into the carbon framework of porous carbons may have a detectable influence on the surface chemical composition and the electron cloud density encircling the carbon skeleton. This, in turn, improves the interaction

Received: December 27, 2023
Revised: February 6, 2024
Accepted: February 15, 2024
Published: February 26, 2024

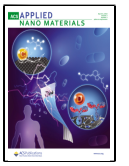

https://doi.org/10.1021/acsanm.3c06239
ACS Appl. Nano Mater. 2024, 7, 5434−5441

between CO_2 and the carbon surface, hence boosting the overall effectiveness of CO_2 capture.[29−35] S- and N-doped porous carbon materials have recently been widely investigated for the CO_2 uptake.[32,33,36−38] Although N-doped porous carbon materials have advantages, such as thermal stability, chemical binding, and enhancing uptake capacity in CO_2 capture, they also have disadvantages. For example, the incorporation of polar nitrogen functionalities into N-doped porous carbon structures can induce heightened hydrophilicity within the material, while this elevated hydrophilicity facilitates enhanced hydrogen bonding between the surface and water molecules, it concurrently raises the prospect of entrapment for water molecules within confined micropores.[39] This phenomenon can thereby lead to a diminution in the overall efficiency of CO_2 catching, particularly when confronted with scenarios marked by elevated humidity levels.[40,41] Sulfones, sulfoxides, and sulfonic acids have been identified for their ability to attract CO_2 through polar interactions and hydrogen bonding.[42,43] Sulfur's larger size relative to carbon introduces strain-induced defects that enhance CO_2 trapping by localizing charges. The polarizable d-orbitals and lone pair of electrons in sulfur enable effective interaction with CO_2's oxygen atoms, while their exceptional pore utilization boosts CO_2 extraction.[44]

S-doped porous nanocarbon (SDC) materials have attracted considerable scholarly interest concerning their applicability in the realm of CO_2 sequestration, primarily attributed to their distinctive physicochemical attributes. The integration of sulfur functionalities into carbon matrices introduces a degree of structural heterogeneity alongside active centers that have the potential to substantially augment the uptake capacities pertinent to CO_2. The distinct electronic configuration inherent to sulfur dopants serves to facilitate heightened intermolecular interactions with CO_2 species, thereby instigating an elevation in uptake affinities.[45] Concurrently, the introduction of sulfur moieties may engender a consequential alteration in the surface chemistry of the carbon substrate, potentially inducing shifts in surface polarity and wettability, thereby engendering a modulation of the material's CO_2 sorption proclivity. The enhanced porosity characteristic of SDC materials, frequently engendered via pyrolytic procedures, engenders supplementary location for the physisorption of CO_2 molecules, therein contributing substantively to an overarching amplification in the CO_2 uptake capacity. Mastery of the intricate nexus between sulfur doping, morphological porosity, and surface reactivity is of cardinal import, given its propensity to mold SDC materials in a manner that optimizes the efficiency of CO_2 capture.[46] For this reason, the inquiry into the attributes of SDC materials emerges as a vanguard avenue within the ambit of CO_2 capture methodologies, bearing relevance in the amelioration of contemporary ecological exigencies. SDCs have been prepared by high-temperature pyrolysis using various sulfur-containing polymers as raw materials such as poly(styrene-divinylbenzene),[47] dipotassium anthraquinone-1,8 disulfonate,[48] poly(sodium 4-styrenesulfonate),[49] thienyl-based polymer,[35] and poly(ether ketone).[50]

This inquiry proposes a thorough and environmentally responsible technique for manufacturing SDCs employing potassium persulfate (PP) as a sulfur dopant and coconut shell, a generally accessible biomass material, as the precursor. The intrinsic availability of coconut shells, a byproduct from the food sector, puts them as an economically effective biomass source characterized by cellulose, hemicellulose, and lignin content. Subjecting these components to high-temperature calcination creates highly organized, porous nanocarbons. The technology adopted here is a one-step synthesis procedure, whereby carbonized coconut shells function as the carbon precursor and PP performs a dual role as both the activator and sulfur supplier. This unusual technique stands out for its explicit avoidance of extra toxic and corrosive sulfur sources, such as H_2S or SO_2, and the deliberate absence of corrosive activation agents like KOH, H_3PO_4, or NaOH. By sidestepping these conventionally utilized ingredients, our new technique not only bolsters the environmental sustainability of the synthesis process but also coincides with a larger ideology of eco-friendly practices in the area of porous nanocarbon production.

2. SYNTHESIS AND CHARACTERIZATION

SDCs were synthesized through a one-pot approach, where carbonized coconut shell (C) served as the carbon precursor and both activation and sulfur incorporation were achieved using PP. For the preparation procedure, a mass ratio of PP to C was selected as 1, 2, and 3, while the activation temperatures were set at either 700 or 750 °C, depending on the case. Nitrogen protected the pyrolysis process. The samples when prepared were allocated as C-PP-X-Y, in which X and Y denote the activation temperature and mass ratio of PP to C, respectively. The yield for these SDCs varies from 81.4 to 25.1%, which declines with increasing activation temperature and PP concentration. Detailed information regarding the preparation of materials, physical characterization, and analysis of CO_2 adsorption can be accessed in the Supporting Information.

3. RESULTS AND DISCUSSION

3.1. Exploring Phase Structure, Morphology, and Surface Chemistry. The scanning electron microscopy (SEM) images in Figure 1 depict the precursor (C) and the optimal CC-P-750-1 sample. Both samples consist of irregular small carbon particles with a surface displaying uneven morphology. In comparison with C, CC-P-750-1, which were activated with PP, exhibited more voids and randomly scattered surface holes. Notably, the CC-P-750-1 appears rougher surface compared to C, most probably owing to

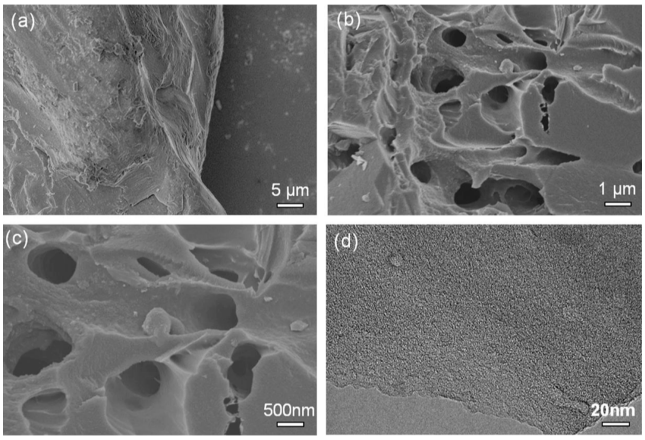

Figure 1. SEM image of (a) C, (b), and (c) CC-P-750-1 and TEM image of (d) CC-P-750-1.

https://doi.org/10.1021/acsanm.3c06239
ACS Appl. Nano Mater. 2024, 7, 5434−5441

Table 1. Pore Structure, Elemental Composition, and CO_2 Sorption Characteristics in SDCs

sample	S_{BET}[a] (m^2/g)	V_0[b] (cm^3/g)	V_t[c] (cm^3/g)	V_n[d] (cm^3/g)	C (wt %)	H (wt %)	N (wt %)	S (wt %)	CO_2 uptake (mmol/g) 25 °C	CO_2 uptake (mmol/g) 0 °C
C				0.10	84.77	3.20	0.42	0.28	0.26	0.43
C-PP-700-1	427	0.18	0.16	0.24	92.99	1.61	0.52	2.63	2.20	2.89
C-PP-700-2	511	0.22	0.19	0.27	89.32	1.74	0.63	2.86	2.39	3.05
C-PP-700-3	642	0.29	0.24	0.31	90.32	1.93	0.57	3.15	2.45	3.31
C-PP-750-1	581	0.26	0.23	0.43	88.00	1.44	0.62	1.23	2.56	3.77
C-PP-750-2	849	0.48	0.36	0.26	89.32	1.21	0.78	1.98	2.29	3.20
C-PP-750-3	866	0.56	0.49	0.37	90.14	0.91	0.84	2.73	1.59	2.35

[a]Surface area was calculated using the BET method at P/P_0 = 0.005−0.05. [b]Total pore volume at P/P_0 = 0.99. [c]Evaluated by the t-plot method. [d]Pore volume of narrow micropores (<1 nm) obtained from the CO_2 adsorption data at 0 °C.

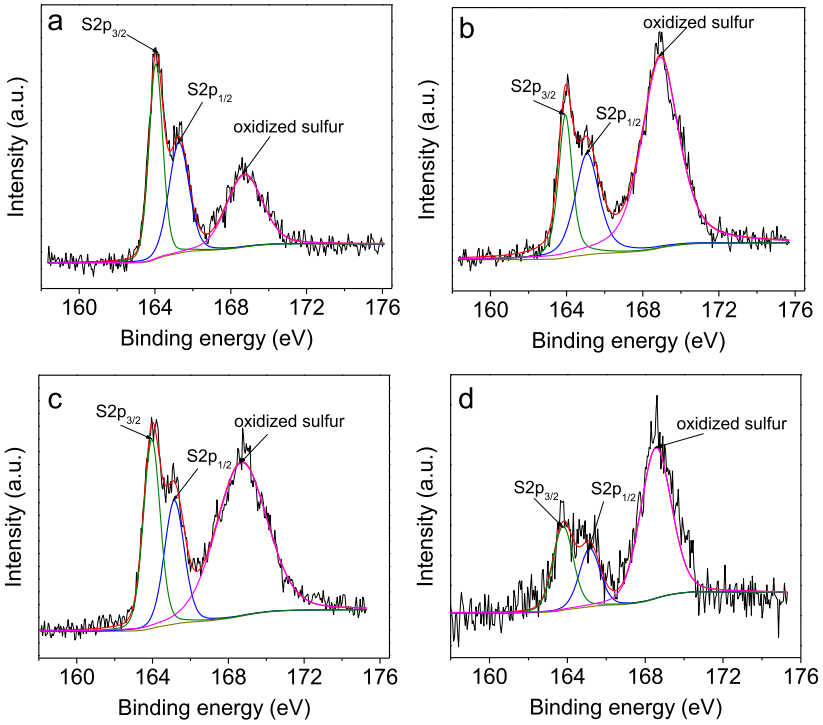

Figure 2. XPS S 2p spectra for (a) C-PP-700-3, (b) C-PP-750-1, (c) C-PP-750-2, and (d) C-PP-750-3.

interactions between the PP and carbon precursors that led to changes in the pore structure and the formation of uneven surfaces. To delve deeper into the exploration, the transmission electron microscopy (TEM) depiction in Figure 1d offers a direct view of the sample's worm-like microscale pore configuration, unveiling its microscale pore arrangement. The considerable abundance of these micropores proves highly advantageous in CO_2 adsorption, as elucidated in previous research.[51,52] To ensure the evaluation of the phase structure of the CC-P-750-1 sample, powdered X-ray diffraction (XRD) characterization was employed. The XRD pattern depicted in Figure S1 (Supporting Information) demonstrates that the carbon has an amorphous structure, with two wide peaks at around 22 and 43°.

Table 1 illustrates the elemental makeup of C and C-PP-X-Y. The carbon content of C is 84.77 wt %, accompanied by 3.20 wt % hydrogen, and trace quantities of nitrogen (0.42 wt %) and sulfur (0.28 wt %). In the C-PP-X-Y samples subjected to PP activating, a substantial rise was observed in the carbon and sulfur content. For instance, in sample C-PP-750-1, the sulfur content was approximately 10-fold that of C. This observation underscores the successful integration of sulfur atoms into the carbon material following the activating process. It is worth noting that the sulfur content was decreased when the activation temperature was from 700 to 750 °C. In essence, the composition of carbon, oxygen, and sulfur within the samples exhibited dependence on the activation temperature. At the same time, it was found that the increase in PP dosage was beneficial for the S-doping. To gain better knowledge regarding surface chemical characteristics concerning S-doping, an X-ray photoelectron spectroscopy (XPS) study was performed for certain typical C-PP-X-Y carbons. The high-resolution S 2p spectra of C-PP-700-3, C-PP-750-1, C-PP-750-2, and C-PP-750-3 samples are illustrated in Figure 2. These spectra displayed two main peaks; (i) oxidized sulfur (appeared on 168.2 ± 0.3 eV) and (ii) neutral sulfur (C−S−C species) that consist of thiophenic structures together with neighboring carbon atoms (163.8 ± 0.3 and 165.0 ± 0.3 eV, corresponding states of S $2p_{3/2}$, S $2p_{1/2}$).[50,53] Specifically, thiophene-S corresponds to sulfur in a non-oxidized state, whereas SO_x (x = 2 and 3) corresponds to sulfur in an oxidized state. The detailed quantities of different S species for these

https://doi.org/10.1021/acsanm.3c06239
ACS Appl. Nano Mater. 2024, 7, 5434−5441

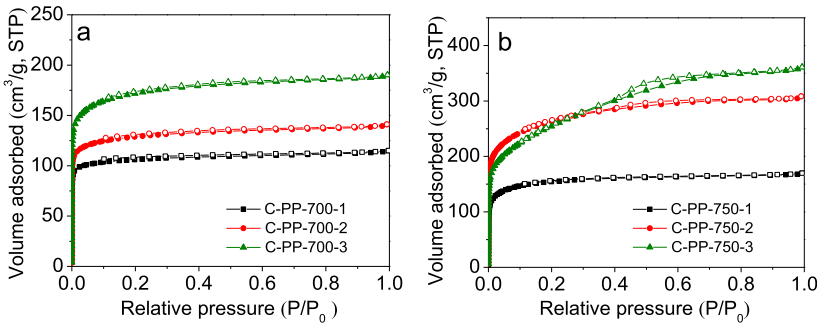

Figure 3. Sorption isotherms of nitrogen for S-enriched carbon-based adsorbents synthesized at (a) 700 °C and (b) 750 °C. Desorption and adsorption branches are, respectively, illustrated with empty and filled symbols.

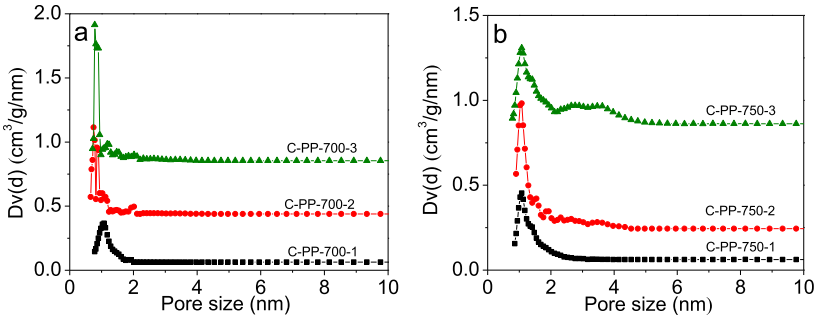

Figure 4. Distribution of pore diameters examined for S-doped carbons synthesized at (a) 700 °C and (b) 750 °C.

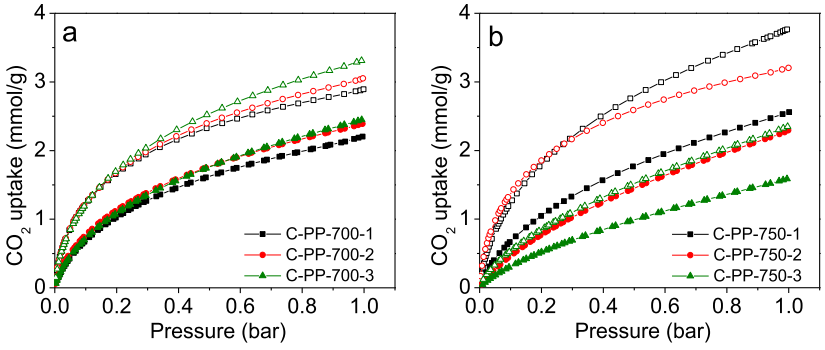

Figure 5. CO_2 adsorption isotherms at 25 °C (filled) and 0 °C (empty) for S-doped carbon adsorbents synthesized at (a) 700 °C and (b) 750 °C.

carbons can be found in Table S1 of the Supporting Information. The XPS analysis provided conclusive evidence that sulfur within the porous nanocarbon material, obtained through PP activation, is predominantly distributed within the carbon matrix in different states, which results in high CO_2 adsorption performance.

3.2. Characteristics of Textual Porosity. The porous features of the C-PP-X-Y materials, as indicated by nitrogen adsorption−desorption isotherms produced by a Beishide 3H-2000PS gas analyzer (Figure 3), coincide with the standard type I-shaped isotherms suggested by the International Union of Pure and Applied Chemistry (IUPAC). The N_2 adsorption isotherms demonstrate a fast rise at low relative pressures ($P/P_0 < 0.1$), suggesting that the fundamental pore structure of the produced SDCs is constituted of micropores. It is noteworthy that discrete hysteresis loops are formed in the P/P_0 range of 0.2 to 0.4 for the CC-P-750-2 and CC-P-750-3 samples as the relative pressure rises, suggesting the presence of mesopores. The pore size distribution curves given in Figure 4 demonstrate that the pore sizes of the S-doped carbon adsorbents are largely concentrated within the range of 0.8 to 1.2 nm, with the most pronounced peak intensity found at 1.1 nm for most samples. On the other hand, the C-PP-750-3 sample presents a wide mesopore peak at the 2−4 nm range. The textural characteristics of the carbon adsorbents are summarized in Table 1. The BET surface area values range from 427 to 866 $m^2\ g^{-1}$, and total pore volume values range from 0.18 to 0.56 $cm^3\ g^{-1}$. Among the samples, C-PP-750-3 exhibited the highest surface area (S_{BET}) of 866 $m^2\ g^{-1}$ and the largest total pore volume (V_t) of 0.56 $cm^3\ g^{-1}$. Generally speaking, as the activating temperature increases, the textural features of the C-PP-X-Y samples develop. A similar trend occurs for the amount of the activating agent, where the higher amount of PP results in induced pore characteristics. This was attributed to complete PP decomposition, leading to open excess pore channels and the release of CO_2 and CO gases from the structure, by leaving an open pore framework.

From former studies, it was recommended that the narrow micropore (<1 nm) was the main factor in deciding the CO_2 adsorption capacity under atmospheric pressure conditions (1

https://doi.org/10.1021/acsanm.3c06239
ACS Appl. Nano Mater. 2024, 7, 5434−5441

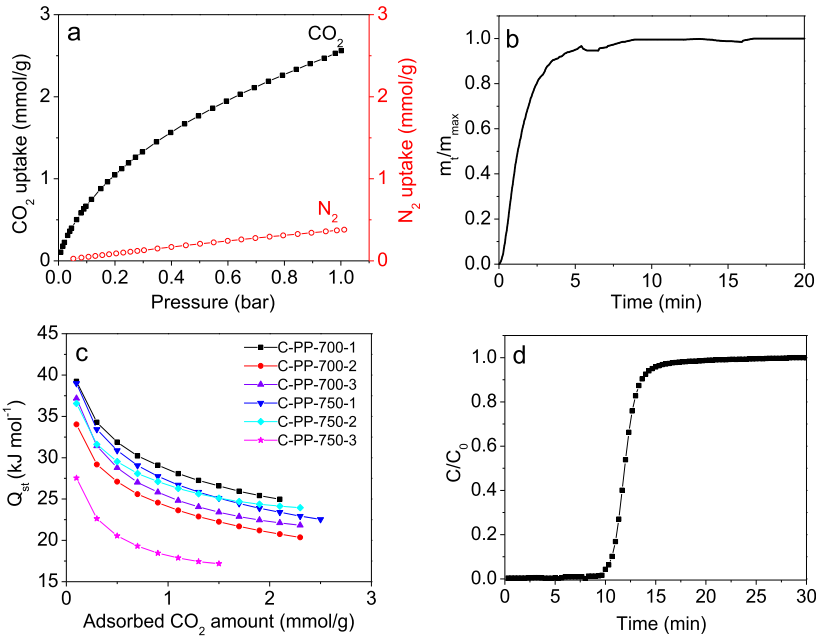

Figure 6. (a) C-PP-750-1 N_2 and CO_2 adsorption isotherms at 1 bar and 298 K, (b) CO_2 adsorption kinetics for C-PP-750-1 at 298 K, (c) isosteric heat of adsorption across all sorbents, and (d) breakthrough curves of C-PP-750-1 under adsorption conditions: 298 K adsorption temperature, 10 mL/min gas flow rate, 10 vol % inlet CO_2 concentration, and 1 bar gas pressure.

bar) at 25 °C.[51,52] In the current inquiry, the estimation of narrow micropore volumes (V_n) for C-PP-X-Y was followed by the application of the Dubinin−Radushkevich (D−R) equation, leveraging the CO_2 adsorption data at 0 °C. Table 1 delineates the detected V_n values throughout these specimens, displaying a range stretching from 0.24 to 0.43 cm^3/g.

3.3. CO_2 Adsorption Evaluation. The CO_2 adsorption analysis of the C-PP-X-Y samples was conducted at both 0 and 25 °C, spanning a pressure range of up to 1 bar. The CO_2 adsorption isotherms displayed in Figure 5 exhibit the notable influence of the chemical reaction conditions on the adsorption capacity of each sample. It has been observed the adsorption capacity exhibited an upward trend as the pressure increased. Additionally, Figure 5 illustrates that the CO_2 adsorption capacity increased as the test temperature decreased from 25 to 0 °C, suggesting the exothermic nature of the CO_2 adsorption process. It has been noted that there is no direct trend between the PP/C ratio and the CO_2 capture capacity. At 700 °C, as the $K_2S_2O_8$ amount rises, the CO_2 capture capacity decreases. On the other hand, the opposite trend has been observed at the activating temperature of 750 °C. An indefinite changing trend between activation temperature and CO_2 capture capacity was also found. When the PP/C ratio was 1, the CO_2 uptake increased with increasing activation temperature, while the CO_2 adsorption capacity decreased with increasing activation temperature under the PP/C ratio of 2 and 3. Remarkably, the C-PP-750-1 sample demonstrated the highest CO_2 adsorption capacity among the samples, boasting 3.77 mmol g^{-1} at 0 °C and 2.56 mmol g^{-1} at 25 °C. At 0.15 bar, the maximum CO_2 uptake for this series of carbons are 1.65 mmol g^{-1} at 0 °C and 0.96 mmol g^{-1} at 25 °C, respectively. Based on Table 1, though C-PP-750-1 has moderate S_{BET} and V_t, along with the lest sulfur functionality, its CO_2 adsorption performance is higher. Upon closer examination, it becomes apparent that the predominant factors governing the CO_2 uptake are the copious presence of narrow microporous structures (the highest V_n for the C-PP-750-1). On the other hand, when comparing C-PP-750-3 with C-PP-700-2 or C-PP-700-3, the C-PP-750-3 has higher V_n than those of C-PP-700-2 and C-PP-700-3 but lower CO_2 uptake. This can be attributed to that the surface composition of C-PP-700-2 and C-PP-700-3 was enriched with higher amounts of sulfur species. This underscores the multifaceted nature of factors influencing adsorption capacity, *i.e.*, both porosity and chemical composition synergize to influence the adsorbent's CO_2 adsorption properties.

It is interesting to underline that the highest CO_2 adsorption capabilities discovered in this inquiry are noticeably lower than those reported for some KOH-activated porous nanocarbons, as shown by earlier investigations,[54,55] However, they demonstrate equivalent or even greater adsorption values when compared with particular carbon materials[56−59] and various other standard CO_2 adsorbents, including COFs,[60] porous polymers,[21] and MOFs.[16] A complete comparison of the uptake of CO_2 among SDC carbons and other solid sorbents is presented in Table S2 of the Supporting Information.

It is widely acknowledged that the efficient separation and capture of CO_2 from flue gas are pivotal criteria for evaluating the potential applications of adsorbents. The CO_2/N_2 selectivity of the sorbents needs to be evaluated. To assess the CO_2/N_2 selectivity, we conducted separate CO_2 and N_2 adsorption tests for the representative C-PP-750-1 under identical conditions at 25 °C and 1 bar (as illustrated in Figure 6a). We utilized the IAST method to predict the CO_2/N_2 selectivity under a gas mixture of CO_2/N_2 (10:90, V/V) at 25 °C and 1 bar. Notably, C-PP-750-1 exhibited an impressive selectivity of 17, surpassing some previously reported carbonaceous adsorbents[24,61] and underscoring its potential for practical CO_2 capture applications.

CO_2 adsorption kinetics is also an important indicator to assess the actual adsorbents. Based on the kinetic analysis shown in Figure 6b, 90% of the saturation adsorption capacity

https://doi.org/10.1021/acsanm.3c06239
ACS Appl. Nano Mater. 2024, 7, 5434−5441

of C-PP-750-1 can be reached within 3.5 min, proving the fast adsorption performance of the as-prepared S-doped carbon adsorbent.

The isosteric heat of adsorption (Q_{st}) serves as a crucial parameter characterizing adsorption performance, offering insights into regeneration energy requirements and the interaction between the adsorbate and adsorbent. Utilizing the Clausius−Clapeyron equation, we calculated Q_{st} values for all the samples from CO_2 adsorption isotherms at 25 and 0 °C (Figure 6c). The observed Q_{st} values ranged from 17 to 39 kJ mol^{-1}, indicating that the CO_2 adsorption mechanism predominantly adheres to a physisorption process. Additionally, the high initial Q_{st} suggests a strong interaction between the adsorbent and the CO_2 molecules. Further exploration revealed that as the level of CO_2 capture increased, Q_{st} values declined until reaching a certain threshold, indicating heterogeneous binding energies within the pores. The relatively lower adsorption heat of these SDCs under high CO_2 loading amounts suggests ease of desorption, the potential for adsorbent recycling, and minimal energy consumption—a favorable combination for practical sulfur-doped carbon adsorbent applications.

We further run a breakthrough experiment to assess the dynamic sorption capacity of the adsorbent; see Figure 6d. The breakthrough experiment comprised subjecting a binary N_2/CO_2 mixture (90:10 v/v) to continuous gas flow at a pressure of 1 bar. Figure 6d clearly illustrates the breakthrough point, occurring roughly 10 min after the commencement of contact between the sorbent and the flowing gas mixture. Under the required test circumstances, the dynamic CO_2 capture capacity (C-PP-750-1) is found to be 0.64 mmol/g, demonstrating good potential for collecting CO_2 from actual flue gas streams. However, it is vital to recognize the presence of moisture in real flue gas, which may lower the CO_2 capture capacity of S-doped carbons owing to the competing adsorption dynamics between CO_2 and H_2O.

To assess the recyclability of the S-doped carbonaceous adsorbent in CO_2 adsorption, we performed five consecutive CO_2 adsorption/desorption cycles for C-PP-750-1 at 25 °C and 1 bar (Figure 7). Encouragingly, the adsorbent maintained its CO_2 capture capacity across multiple cycles, signifying remarkable reusability and potential for real-world engineering applications.

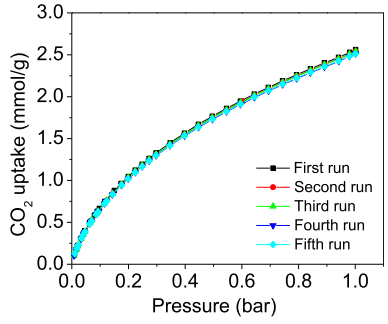

Figure 7. Repetitive CO_2 adsorption testing was conducted on C-PP-750-1.

4. CONCLUSIONS

Within the context of this study, we effectively produced SDCs using the carbonization process of coconut shells, utilizing PP as both an activating agent and a sulfur source. The synthesis process involves systematic adjustments in the pyrolysis temperature, including the range of 700 to 750 °C, and modulation of the PP/C ratio at 1, 2, and 3. This deliberate control over synthesis settings created a varied variety of porous nanocarbon materials, showing a spectrum of features. Notably, the materials displayed a maximum surface area of 866 m^2 g^{-1}, paired with a pore volume of 0.56 cm^3 g^{-1}. Furthermore, the heteroatom composition within the materials was finely adjustable. Under the working settings of 1 bar and temperatures of 0 and 25 °C, the ideally constructed C-PP-750-1 adsorbent displayed exceptional CO_2 absorption capabilities, recording values of 3.77 and 2.56 mmol g^{-1}, respectively. This discovery emphasized the significant impact of both the narrow microporosity and sulfur content on increasing the CO_2 sorption capacity. Beyond mere capacity, these sulfur-doped porous carbons demonstrated desirable features, including a favorable isosteric heat of adsorption, quick adsorption kinetics, excellent CO_2/N_2 selectivity, strong cycle stability, and significant dynamic CO_2 capture capacity. Collectively, these outcomes not only present a significant advancement in the production of porous carbon materials endowed with boosted sulfur functionalities but also advocate for a comprehensive exploration of these materials across a spectrum of applications involving gas adsorption and separation. The nuanced tailoring of synthesis parameters and the consequent different characteristics of the materials create pathways for specialized applications in numerous scientific and commercial fields.

■ ASSOCIATED CONTENT

Supporting Information

The Supporting Information is available free of charge at https://pubs.acs.org/doi/10.1021/acsanm.3c06239.

Details for sorbent synthesis, characterization, CO_2 capture system, XRD pattern of C-PP-750-1, contribution of different S species of the samples, and comparison of the CO_2 adsorption capacities for various sorbents (PDF)

■ AUTHOR INFORMATION

Corresponding Authors

Muslum Demir − *Department of Chemical Engineering, Bogazici University, Istanbul 34342, Turkey; TUBITAK Marmara Research Center, Material Institute, Gebze 41470, Turkey;* orcid.org/0000-0001-6842-8124; Email: demirm@alumni.vcu.edu

Xin Hu − *Key Laboratory of the Ministry of Education for Advanced Catalysis Materials, Zhejiang Normal University, Jinhua, Zhejiang 321004, P.R. China;* orcid.org/0000-0002-9851-1049; Phone: 86-151-0579-0257; Email: huxin@zjnu.cn; Fax: 86-579-8228-8269

Authors

Chen Liu − *Key Laboratory of the Ministry of Education for Advanced Catalysis Materials, Zhejiang Normal University, Jinhua, Zhejiang 321004, P.R. China*

Yue Zhi − *Key Laboratory of the Ministry of Education for Advanced Catalysis Materials, Zhejiang Normal University, Jinhua, Zhejiang 321004, P.R. China*

Qiyun Yu − *Key Laboratory of the Ministry of Education for Advanced Catalysis Materials, Zhejiang Normal University, Jinhua, Zhejiang 321004, P.R. China*

Lifeng Tian − *Key Laboratory of the Ministry of Education for Advanced Catalysis Materials, Zhejiang Normal University, Jinhua, Zhejiang 321004, P.R. China*

Suleyman Gokhan Colak − *Department of Biomedical Engineering, Faculty of Engineering and Natural Sciences, Iskenderun Technical University, Hatay 31200, Turkey*

Ahmed A. Farghaly − *Chemical Sciences and Engineering Division, Argonne National Laboratory, Lemont, Illinois 60439, United States; Pritzker School of Molecular Engineering, The University of Chicago, Chicago, Illinois 60637, United States; Chemistry Department, Faculty of Science, Assiut University, Assiut 71516, Egypt;* orcid.org/0000-0001-7948-3700

Linlin Wang − *Key Laboratory of Urban Rail Transit Intelligent Operation and Maintenance Technology and Equipment of Zhejiang Province, College of Engineering, Zhejiang Normal University, Jinhua, Zhejiang 321004, PR China*

Complete contact information is available at: https://pubs.acs.org/10.1021/acsanm.3c06239

Notes

The authors declare no competing financial interest.

■ ACKNOWLEDGMENTS

The Zhejiang Provincial Natural Science Foundation (LY21B070005), the National Undergraduate Training Program for Innovation and Entrepreneurship of China, and the Self-Designed Scientific Research Project of Zhejiang Normal University (no. 2021ZS06) provided financial support.

■ REFERENCES

(1) Sullivan, I.; Goryachev, A.; Digdaya, I. A.; Li, X. Q.; Atwater, H. A.; Vermaas, D. A.; Xiang, C. X. Coupling electrochemical CO_2 conversion with CO_2 capture. *Nat. Catal.* **2021**, *4* (11), 952−958.

(2) Suleman, H.; Fosbøl, P. L.; Nasir, R.; Ameen, M. *Sustainable Carbon Capture: Technologies and Applications*; CRC Press, 2022.

(3) Singh, G.; Lee, J.; Karakoti, A.; Bahadur, R.; Yi, J.; Zhao, D.; AlBahily, K.; Vinu, A. Emerging trends in porous materials for CO(2)capture and conversion. *Chem. Soc. Rev.* **2020**, *49* (13), 4360−4404.

(4) Guo, Y. F.; Tan, C.; Sun, J.; Li, W. L.; Zhang, J. B.; Zhao, C. W. Porous activated cartbons derived from waste sugarcane bagasse for CO_2 adsorption. *Chem. Eng. J.* **2020**, *381*, 122736.

(5) Wang, J.; Zhang, P. X.; Liu, L.; Zhang, Y.; Yang, J. F.; Zeng, Z. L.; Deng, S. G. Controllable synthesis of bifunctional porous carbon for efficient gas-mixture separation and high-performance supercapacitor. *Chem. Eng. J.* **2018**, *348*, 57−66.

(6) Ma, C.; Lu, T.; Shao, J.; Huang, J.; Hu, X.; Wang, L. Biomass-derived nitrogen and sulfur co-doped porous carbons for efficient CO_2 adsorption. *Sep. Purif. Technol.* **2022**, *281*, 119899.

(7) Shi, J.; Cui, H.; Xu, J.; Yan, N.; Liu, Y. Design and fabrication of hierarchically porous carbon frameworks with Fe_2O_3 cubes as hard template for CO_2 adsorption. *Chem. Eng. J.* **2020**, *389*, 124459.

(8) Shi, S.; Liu, Y. Nitrogen-doped activated carbons derived from microalgae pyrolysis by-products by microwave/KOH activation for CO_2 adsorption. *Fuel* **2021**, *306*, 121762.

(9) Demir, M.; Doguscu, M. Preparation of Porous Carbons Using NaOH, K_2CO_3, Na_2CO_3 and $Na_2S_2O_3$ Activating Agents and Their Supercapacitor Application: A Comparative Study. *Chemistryselect* **2022**, *7* (4), No. e202104295.

(10) Rehman, A.; Nazir, G.; Yop Rhee, K.; Park, S.-J. A rational design of cellulose-based heteroatom-doped porous carbons: Promising contenders for CO_2 adsorption and separation. *Chem. Eng. J.* **2021**, *420*, 130421.

(11) Rehman, A.; Park, S.-J. From chitosan to urea-modified carbons: Tailoring the ultra-microporosity for enhanced CO_2 adsorption. *Carbon* **2020**, *159*, 625−637.

(12) Yu, Q.; Bai, J.; Huang, J.; Demir, M.; Farghaly, A. A.; Aghamohammadi, P.; Hu, X.; Wang, L. One-Pot Synthesis of Melamine Formaldehyde Resin-Derived N-Doped Porous Carbon for CO_2 Capture Application. *Molecules* **2023**, *28* (4), 1772.

(13) Huang, J.; Bai, J.; Demir, M.; Hu, X.; Jiang, Z.; Wang, L. Efficient N-Doped Porous Carbonaceous CO_2 Adsorbents Derived from Commercial Urea-Formaldehyde Resin. *Energy Fuels* **2022**, *36* (11), 5825−5832.

(14) Lu, T.; Bai, J.; Demir, M.; Hu, X.; Huang, J.; Wang, L. Synthesis of potassium Bitartrate-derived porous carbon via a facile and Self-Activating strategy for CO_2 adsorption application. *Sep. Purif. Technol.* **2022**, *296*, 121368.

(15) Lu, T.; Ma, C.; Demir, M.; Yu, Q.; Aghamohammadi, P.; Wang, L.; Hu, X. One-pot synthesis of potassium benzoate-derived porous carbon for CO_2 capture and supercapacitor application. *Sep. Purif. Technol.* **2022**, *301*, 122053.

(16) Millward, A. R.; Yaghi, O. M. Metal-Organic Frameworks with Exceptionally High Capacity for Storage of Carbon Dioxide at Room Temperature. *J. Am. Chem. Soc.* **2005**, *127* (51), 17998−17999.

(17) Yu, J.; Xie, L.-H.; Li, J.-R.; Ma, Y.; Seminario, J. M.; Balbuena, P. B. CO_2 Capture and Separations Using MOFs: Computational and Experimental Studies. *Chem. Rev.* **2017**, *117* (14), 9674−9754.

(18) Kumar, S.; Srivastava, R.; Koh, J. Utilization of zeolites as CO_2 capturing agents: Advances and future perspectives. *J. CO2 Util.* **2020**, *41*, 101251.

(19) Sekizkardes, A. K.; Budhathoki, S.; Zhu, L.; Kusuma, V.; Tong, Z.; McNally, J. S.; Steckel, J. A.; Yi, S.; Hopkinson, D. Molecular design and fabrication of PIM-1/polyphosphazene blend membranes with high performance for CO_2/N_2 separation. *J. Membr. Sci.* **2021**, *640*, 119764.

(20) Zhu, D.; Zhu, Y.; Chen, Y.; Yan, Q.; Wu, H.; Liu, C.-Y.; Wang, X.; Alemany, L. B.; Gao, G.; Senftle, T. P.; Peng, Y.; Wu, X.; Verduzco, R. Three-dimensional covalent organic frameworks with pto and mhq-z topologies based on Tri- and tetratopic linkers. *Nat. Commun.* **2023**, *14* (1), 2865.

(21) Sun, L.-B.; Kang, Y.-H.; Shi, Y.-Q.; Jiang, Y.; Liu, X.-Q. Highly Selective Capture of the Greenhouse Gas CO_2 in Polymers. *ACS Sustain. Chem. Eng.* **2015**, *3* (12), 3077−3085.

(22) Shao, L.; Li, Y.; Huang, J.; Liu, Y.-N. Synthesis of Triazine-Based Porous Organic Polymers Derived N-Enriched Porous Carbons for CO_2 Capture. *Ind. Eng. Chem. Res.* **2018**, *57* (8), 2856−2865.

(23) Sang, Y. F.; Cao, Y. W.; Wang, L. Z.; Yan, W.; Chen, T. W.; Huang, J. H.; Liu, Y. N. N-rich porous organic polymers based on Schiff base reaction for CO_2 capture and mercury(II) adsorption. *J. Colloid Interface Sci.* **2021**, *587*, 121−130.

(24) Shen, Y. F. Preparation of renewable porous carbons for CO_2 capture - A review. *Fuel Process. Technol.* **2022**, *236*, 107437.

(25) Bai, J. L.; Huang, J. M.; Yu, Q. Y.; Demir, M.; Akgul, E.; Altay, B. N.; Hu, X.; Wang, L. L. Fabrication of coconut shell-derived porous carbons for CO_2 adsorption application. *Front. Chem. Sci. Eng.* **2023**, *17* (8), 1122−1130.

(26) Aydin, H.; Üstün, B.; Kurtan, Ü.; Aslan, A.; Karakus, S. Incorporating Gadolinium Oxide (Gd_2O_3) as a Rare Earth Metal Oxide in Carbon Nanofiber Skeleton for Supercapacitor Application. *Chemelectrochem* **2024**, *11*, No. e202300585.

(27) Ustun, B.; Aydin, H.; Koc, S. N.; Kurtan, U. Thiourea-assisted nitrogen and sulfur dual-doped carbon nanofibers for enhanced supercapacitive energy storage. *J. Mater. Sci. Mater. Electron.* **2023**, *34* (5), 408.

(28) Üstün, B.; Aydın, H.; Koç, S.; Uluslu, A.; Kurtan, Ü. Electrospun polyethylenimine (PEI)-derived nitrogen enriched

carbon nanofiber for supercapacitors with artificial neural network modeling. *J. Energy Storage* **2023**, *73*, 108970.
(29) Aghel, B.; Behaein, S.; Alobaid, F. CO_2 capture from biogas by biomass-based adsorbents: A review. *Fuel* **2022**, *328*, 125276.
(30) Xiao, J.; Yuan, X.; Zhang, T. C.; Ouyang, L.; Yuan, S. Nitrogen-doped porous carbon for excellent CO_2 capture: A novel method for preparation and performance evaluation. *Sep. Purif. Technol.* **2022**, *298*, 121602.
(31) Yuan, X.; Xiao, J.; Yilmaz, M.; Zhang, T. C.; Yuan, S. N, P Co-doped porous biochar derived from cornstalk for high performance CO_2 adsorption and electrochemical energy storage. *Sep. Purif. Technol.* **2022**, *299*, 121719.
(32) Bai, J.; Huang, J.; Yu, Q.; Demir, M.; Kilic, M.; Altay, B. N.; Hu, X.; Wang, L. N-doped porous carbon derived from macadamia nut shell for CO_2 adsorption. *Fuel Process. Technol.* **2023**, *249*, 107854.
(33) Shao, J.; Ma, C.; Zhao, J.; Wang, L.; Hu, X. Effective nitrogen and sulfur co-doped porous carbonaceous CO_2 adsorbents derived from amino acid. *Colloids Surf., A* **2022**, *632*, 127750.
(34) Benzigar, M. R.; Talapaneni, S. N.; Joseph, S.; Ramadass, K.; Singh, G.; Scaranto, J.; Ravon, U.; Al-Bahily, K.; Vinu, A. Recent advances in functionalized micro and mesoporous carbon materials: synthesis and applications. *Chem. Soc. Rev.* **2018**, *47* (8), 2680−2721.
(35) Bai, J.; Huang, J.; Jiang, Q.; Jiang, W.; Demir, M.; Kilic, M.; Altay, B. N.; Wang, L.; Hu, X. Synthesis and characterization of polyphenylene sulfide resin-derived S-doped porous carbons for efficient CO_2 capture. *Colloids Surf., A* **2023**, *674*, 131916.
(36) Bai, J.; Huang, J.; Yu, Q.; Demir, M.; Gecit, F. H.; Altay, B. N.; Wang, L.; Hu, X. One-pot synthesis of self S-doped porous carbon for efficient CO_2 adsorption. *Fuel Process. Technol.* **2023**, *244*, 107700.
(37) Bai, J.; Shao, J.; Yu, Q.; Demir, M.; Nazli Altay, B.; Muhammad Ali, T.; Jiang, Y.; Wang, L.; Hu, X. Sulfur-Doped porous carbon Adsorbent: A promising solution for effective and selective CO_2 capture. *Chem. Eng. J.* **2024**, *479*, 147667.
(38) Shao, J.; Wang, J.; Yu, Q.; Yang, F.; Demir, M.; Altinci, O. C.; Umay, A.; Wang, L.; Hu, X. Unlocking the potential of N-doped porous Carbon: Facile synthesis and superior CO_2 adsorption performance. *Sep. Purif. Technol.* **2024**, *333*, 125891.
(39) Wang, Z.; Goyal, N.; Liu, L. Y.; Tsang, D. C. W.; Shang, J.; Liu, W. J.; Li, G. N-doped porous carbon derived from polypyrrole for CO_2 capture from humid flue gases. *Chem. Eng. J.* **2020**, *396*, 125376.
(40) Petrovic, B.; Gorbounov, M.; Masoudi Soltani, S. Influence of surface modification on selective CO_2 adsorption: A technical review on mechanisms and methods. *Microporous Mesoporous Mater.* **2021**, *312*, 110751.
(41) Zhang, Z.; Cano, Z. P.; Luo, D.; Dou, H.; Yu, A.; Chen, Z. Rational design of tailored porous carbon-based materials for CO_2 capture. *J. Mater. Chem. A* **2019**, *7* (37), 20985−21003.
(42) Kwiatkowski, M.; Policicchio, A.; Seredych, M.; Bandosz, T. J. Evaluation of CO_2 interactions with S-doped nanoporous carbon and its composites with a reduced GO: Effect of surface features on an apparent physical adsorption mechanism. *Carbon* **2016**, *98*, 250−258.
(43) Seredych, M.; Jagiello, J.; Bandosz, T. J. Complexity of CO_2 adsorption on nanoporous sulfur-doped carbons—Is surface chemistry an important factor? *Carbon* **2014**, *74*, 207−217.
(44) Seema, H.; Kemp, K. C.; Le, N. H.; Park, S. W.; Chandra, V.; Lee, J. W.; Kim, K. S. Highly selective CO_2 capture by S-doped microporous carbon materials. *Carbon* **2014**, *66*, 320−326.
(45) Ma, G.; Ning, G.; Wei, Q. S-doped carbon materials: Synthesis, properties and applications. *Carbon* **2022**, *195*, 328−340.
(46) Lu, T. Y.; Bai, J. L.; Huang, J. M.; Yu, Q. Y.; Demir, M.; Kilic, M.; Altay, B. N.; Wang, L. L.; Hu, X. Self-Activating Approach for Synthesis of 2,6-Naphthalene Disulfonate Acid Disodium Salt-Derived Porous Carbon and CO_2 Capture Performance. *Energy Fuels* **2023**, *37*, 3886−3893.
(47) Sun, Y.; Zhao, J.; Wang, J.; Tang, N.; Zhao, R.; Zhang, D.; Guan, T.; Li, K. Sulfur-doped millimeter-sized microporous activated carbon spheres derived from sulfonated poly (styrene−divinylbenzene) for CO_2 capture. *J. Phys. Chem. C* **2017**, *121* (18), 10000−10009.
(48) Cui, H.; Xu, J.; Shi, J.; Zhang, C. Synthesis of sulfur doped carbon from dipotassium anthraquinone-1, 8-disulfonate for CO_2 adsorption. *J. CO2 Util.* **2021**, *50*, 101582.
(49) Su, W.; Yao, L.; Ran, M.; Sun, Y.; Liu, J.; Wang, X. Adsorption properties of N_2, CH_4, and CO_2 on sulfur-doped microporous carbons. *J. Chem. Eng. Data* **2018**, *63* (8), 2914−2920.
(50) Bag, S.; Pal, K. Sulfonated poly (ether ether ketone) based carbon dioxide gas sensor: Impact of sulfonation degree on sensing behavior at different humid condition. *Sens. Actuators, B* **2020**, *303*, 127115.
(51) Presser, V.; McDonough, J.; Yeon, S.-H.; Gogotsi, Y. Effect of pore size on carbon dioxide sorption by carbide derived carbon. *Energy Environ. Sci.* **2011**, *4* (8), 3059−3066.
(52) Sevilla, M.; Fuertes, A. B. Sustainable porous carbons with a superior performance for CO_2 capture. *Energy Environ. Sci.* **2011**, *4* (5), 1765−1771.
(53) Guo, X.; Zhang, G.; Wu, C.; Liu, J.; Li, G.; Zhao, Y.; Wang, Y.; Xu, Y. A cost-effective synthesis of heteroatom-doped porous carbon by sulfur-containing waste liquid treatment: As a promising adsorbent for CO_2 capture. *J. Environ. Chem. Eng.* **2021**, *9* (2), 105165.
(54) Wickramaratne, N. P.; Jaroniec, M. Activated Carbon Spheres for CO_2 Adsorption. *ACS Appl. Mater. Interfaces* **2013**, *5* (5), 1849−1855.
(55) Sethia, G.; Sayari, A. Comprehensive study of ultra-microporous nitrogen-doped activated carbon for CO_2 capture. *Carbon* **2015**, *93*, 68−80.
(56) Yu, Q. Y.; Bai, J. L.; Huang, J. M.; Demir, M.; Altay, B. N.; Hu, X.; Wang, L. L. One-Pot Synthesis of N-Rich Porous Carbon for Efficient CO_2 Adsorption Performance. *Molecules* **2022**, *27* (20), 6816.
(57) Ligero, A.; Calero, M.; Perez, A.; Solis, R. R.; Munoz-Batista, M. J.; Martin-Lara, M. A. Low-cost activated carbon from the pyrolysis of post-consumer plastic waste and the application in CO_2 capture. *Process Saf. Environ. Prot.* **2023**, *173*, 558−566.
(58) Wu, R.; Bao, A. L. Preparation of cellulose carbon material from cow dung and its CO_2 adsorption performance. *J. CO2 Util.* **2023**, *68*, 102377.
(59) Wang, Y. F.; Xu, J. H.; Lin, X. L.; Wang, B. L.; Zhang, Z. G.; Xu, Y. S.; Suo, Y. G. Facile synthesis of MOF-5-derived porous carbon with adjustable pore size for CO_2 capture. *J. Solid State Chem.* **2023**, *322*, 123984.
(60) Furukawa, H.; Yaghi, O. M. Storage of Hydrogen, Methane, and Carbon Dioxide in Highly Porous Covalent Organic Frameworks for Clean Energy Applications. *J. Am. Chem. Soc.* **2009**, *131* (25), 8875−8883.
(61) Karimi, M.; Shirzad, M.; Silva, J. A. C.; Rodrigues, A. E. Biomass/Biochar carbon materials for CO_2 capture and sequestration by cyclic adsorption processes: A review and prospects for future directions. *J. CO2 Util.* **2022**, *57*, 101890.

https://doi.org/10.1021/acsanm.3c06239
ACS Appl. Nano Mater. 2024, 7, 5434−5441